Citrobacter sp. Y3 Harboring a Novel Gene HBCD-hd-1 Mineralizes Hexabromocyclododecane (HBCD) with New Metabolic Pathways Based on Multi-omics Characterization

Xingxing Peng (pengxx6@mail.sysu.edu.cn)
Sun Yat-sen University
Tianyu Li
Sun Yat-sen University
Qihang Zheng
Sun Yat-sen University
Yingyuan Lu
Sun Yat-sen University
Yuzhe He
Sun Yat-sen University
Yetao Tang
Sun Yat-sen University
Rongliang Qiu
South China Agricultural University

Research Article

Keywords: Hexabromocyclododecane, Mineralization, Multi-omics, Catabolic pathway, Identification of functional gene

Posted Date: July 1st, 2022

DOI: https://doi.org/10.21203/rs.3.rs-1782615/v1

Abstract

Background: Hexabromocyclododecane (HBCD) is a typical persistent organic pollutant that is widely detected in the environment. Until now, a microorganism resource that can degrade and even completely mineralizing HBCD is lacking.

Results: By stable isotope analysis, we found that the *Citrobacter* sp. strain Y3 can use ^{13}C-HBCD as its sole carbon source and degrade or even mineralize it to $^{13}CO_2$ with a maximum conversion rate of 100% in approximately 14 days. Genomics, proteomics, and metabolomics were used to study the catabolic pathway of HBCD biodegradation by strain Y3. Several enzymes reportedly involved in the degradation of HBCD were identified in the strain Y3. A new functional gene named *HBCD-hd-1* encoding a haloacid dehalogenase was cloned and heterologously expressed in *Escherichia coli*. The recombinant *E. coli* transformed the typical intermediate 4-bromobutyric acid (4-BBA) to 4-hydroxybutanoic acid (4-HDBA) and showed excellent degradation performance on HBCD with a degradation rate of 100% in only 2 days. Meanwhile, HBCD was well debrominated by the recombinant *E. coli*, because nearly 100% bromine ions were detected by ion chromatograph (IC) in vitro.

Conclusion: This is the first report on the degradation function of haloacid dehalogenase in HBCD treatment. Strain Y3 can potentially degrade brominated flame retardants such as HBCD especially in a low-nutrient environment.

Introduction

Hexabromocyclododecane (HBCD), as a typical brominated flame retardant, is easily released to the environment during its manufacture, storage, and use. HBCD production is over 31,000 metric tons in China, Europe, and United States, according to the latest estimation on its global production [1]. Considering its persistent, long-distance migration ability, bioaccumulation effect, and toxicity in wildlife and human bodies [2, 3], HBCD has been listed by the Stockholm Convention as persistent organic pollutant (POP) in 2013 and can only be used under strict regulatory rules [4]. It has been frequently and widely detected in air, water, sediment, soil, and organisms [5]. HBCD residues have attracted much public attention, and its remediation in the environment has become urgent and necessary. Biodegradation plays an important role in HBCD removal in soil, wastewater treatment plants, and sediment [6]. Acquiring enough microbial resource to treat HBCD and understanding its biodegradation mechanism has become essential.

Previous studies in this area reported the removal efficiency and degradation pathway of HBCD in activated sludge and soil [6, 7]. In addition, several pure cultures that could degrade HBCD have been isolated from the environment [6], including aerobic bacteria *Bacillus* sp. HBCD-sjtu [8], *Pseudomonas* sp. GJY [9], and *Pseudomonas aeruginosa* HS9 [10] and anaerobic bacteria *Sphingobium chinhatense* IP26 [11] and *Achromobacter* sp. HBCD-1 [12]. All these pure cultures could partly convert HBCD to typical intermediates, including pentabromocyclododecanols (PBCDOHs), tetrabromocyclododecadiols

(TBCDDOHs), and 1,5,9-cyclododecatriene (CDT), by debromination. Some cultures can convert the intermediates by hydrolyzation. However, most HBCD-degrading bacteria isolated to date cannot use HBCD as a sole carbon source and therefore cannot degrade it into basic biomass and CO_2. In addition, studies about HBCD mineralization by pure cultures have not been performed. If not completely mineralized, then the intermediates may lead to secondary pollution during the degradation process.

Known enzymes involved in HBCD conversion, including gamma-hexachlorocyclohexane dehydrochlorinase (LinA), dehydrochlorinase, haloalkane dehalogenase (LinB), and haloalkane dehalogenase (DhaA), were verified in vitro and studied in detail [13–15]. LinA converts HBCDs to pentabromocyclododecene (PBCDE) [16]. It has several variants, such as LinA1 and LinA2, which share about 90% similarity in their amino acid sequences [17]. Both of these variants originated from *Sphingobium indicum* B90A. LinB, which can be isolated from *S. chinhatense* IP26, can initially catalyze HBCD to become PBCDOHs; it can further catalyze it to become TBCDDOHs [18]. Although a LinB homology of enzyme DehHZ1 extracted from *B.* sp. HBCD-sjtu transformed HBCD, different products of CDT were determined. Despite that HBCD-degrading enzymes of dehydrochlorinase and DhaA have been identified, other clades of enzymes for HBCD removal are still lacking. In particular, enzymes responsible for the later mineralization after CDT degradation are completely unknown.

Previously, we have confirmed that *Citrobacter* sp. Y3 could transform HBCD using sodium citrate as additional carbon source [19]. In the present work, with the stable isotope labelling ^{13}C-HBCD (α-, β-, and γ-HBCD), the degradation efficiency and mineralization rate of α-, β-, and γ-HBCD by strain Y3 were studied (Fig. 1). The detailed genomic and proteomic characterization of strain Y3 was obtained by high-throughput sequencing technique. The degradation pathway of HBCD was rebuilt by identifying intermediates through ultra-performance liquid chromatography-quadrupole-time-of-flight-mass spectrometry (UPLC-Q-TOF-MS), the annotation of functional genes, and protein expression by omics. A hypothetical gene *HBCD-hd-1* that encodes a new dehalogenase was cloned and identified. It possessed high performance on HBCD and its intermediates of 4- bromobutyric acid (4-BBA).

Results And Discussion

Mineralization of HBCD by strain Y3

The strain Y3 could effectively bio-transform HBCD, including its isomers, i.e., α-, β-, and γ-HBCD [20]. It could utilize ^{13}C-HBCD (α-, β-, and γ-HBCD) as sole carbon source and degrade it to $^{13}CO_2$ to various extents within a certain timeframe (Fig. 2). The degradation rate of β-^{13}C-HBCD was approximately 100% in 12 days, whereas those of α-^{13}C-HBCD and γ-^{13}C-HBCD were approximately 80% and 95%, respectively. The removal rates of ^{13}C-HBCD diastereomers were in the following order: β- > γ- > α-^{13}C-HBCD. This order was consistent with that obtained by Heeb et al [11]. This was different from results of another study, in which the degradation rates of α- and β-HBCD were faster than that of γ-HBCD [9]. The produced $^{13}CO_2$ by β-^{13}C-HBCD mineralization reached approximately 8.2 ppm within 18 days, which indicated that the

mineralization rate reached 100%. The concentrations of $^{13}CO_2$ produced by γ- and α-^{13}C-HBCD were 7.5 and 6.7 ppm, respectively. The conversion to $^{13}CO_2$ was 91.5% and 81.7%, respectively. The HBCD mineralization rates of the three diastereomers were in the following order: β- > γ- > α-HBCD. The α-HBCD, which had the lowest degradation, was the most stable, because of its physico-chemical properties, such as water solubility and octanol-water partition coefficient [20, 21]. It is the predominant HBCD diastereoisomer in biological tissues and can be converted from β- and γ-HBCD [22].

Genomic characterization

DNA was extracted from *Citrobacter* sp. Y3 and subjected to whole-genome sequencing. The genome of *Citrobacter* sp. Y3 consisted of one circular chromosome (5 246 113 bp) and two circular plasmids (34 341 and 89 705 bp). The GC content of strain *Citrobacter* sp. Y3 was 54.19%. It contained 5240 protein-coding genes, as shown in Table S2. The assembly of strain Y3 genome yielded one contig with 76 241 reads and with a mean read length of 12 685 bp and an N50 contig length of 4 542 216 bp. The chromosome and plasmid of strain Y3 contained 5240 ORFs, of which 5092 (97%) were putative coding sequences (CDS). There were 22 RNA genes (5s, 16s, and 23s rRNA genes), 84 tRNA genes, and 59 ncRNA genes (Fig. S1).

Overview of proteomics

Proteomic analysis identified a total of 5006 proteins, which were equivalent to the predicted 95.5% of CDS. Of these, 492 proteins were upregulated and 670 were downregulated in the presence of HBCD (Fig. 3a). The number of proteins quantified and differentially abundant by less than 2-fold [$-1.0 \leq \log_2$ (fold abundance) ≤ 1.0, $p \leq 0.05$] in response to HBCD are shown in Fig. 3b. The shaded areas represent proteins with more than 2-fold differential abundance [$-1.0 \geq \log_2$ (fold abundance) or $\log_2$ (fold abundance) ≥ 1.0, $p \leq 0.05$]. All identified proteins were divided into three categories in Fig. 3c, namely, biological processes (BP), cellular components (CC), and metabolic functions (MF). The presence of HBCD led to the overexpression of proteins related to ionic glutamate receptor active protein, arginine biosynthesis process protein, and ribosome. Strain Y3 can completely biodegrade HBCD. Thus, the metabolism process may involve three metabolic pathways, namely, carbon metabolism (CM), energy metabolism (EM), and xenobiotics metabolism (XM). According to further analysis based on the functional annotation of KEGG annotated genes, 45 proteins related to CM (Table S3), EM (Table S4), and XM (Table S5) were screened out from the 492 upregulated proteins. As shown in Fig. 3d, 26 upregulated proteins were related to CM. The abundance of 11 kinds of upregulated proteins closely related to the process of EM more than tripled. XM proteins were most likely involved with HBCD degradation. Thus, particular research focus was given to the study of XM. Among them, 11 kinds of upregulated proteins were found. The proteins involved in dehalogenation mainly included haloacid dehalogenase (DhaG) [23], DhaA [24], LinA [25], and LinB [14]. Some proteins, such as glutathione S-transferase (GST) [26] and cytochrome P450 (CYP450) [27], were found in other metabolism pathways; they probably participated in the debromination of HBCD.

Reconstruction of HBCD catabolic pathway using genomic, proteomic, and metabolic analyses

Seventeen biodegradation intermediates were identified by UHPLC-MS/MS (Table S6 and Fig. S2). According to the analysis of genomic, proteomic, and metabolic intermediates, HBCD degradation pathways by strain Y3 were proposed, as shown in Fig. 4. Obviously, HBCD debrominated via two pathways. The first pathway involved the detaching of bromine (Br) atoms from the compound during the process. Some typical products generated by gradual debromination include PBCDE (7.13 min, m/z of 573), tetrabromocyclododecane (TBCD) (9.49 min, m/z of 494), tribromocyclodedecane (TriBCD) (6.42 min, m/z of 413), dibromocyclododecane (DBCD) (1.76 min, m/z of 334), and CDT (4.41 min, m/z of 174). Similar intermediates were found in the degradation of HBCD by other strains of *B.* sp. HBCD-sjtu, *Dehalococcoides mccartyi* 195, and *P. aeruginosa* HS9 [8, 28]. LinA catalyzed dehalogenation processes, including debromination [16, 18, 29]. The expression volume of LinA was upregulated with 1- to 2-fold abundance increase (log_2 of 8.0 to 12.3) after HBCD treatment.

The CDT could be further transformed to intermediates, such as (4Z,8Z)-13-oxabicyclo [10.1.0] trideca-4,8-diene (ECDD) (1.02 min, m/z of 190), cyclododecane (CDDA) (3.76 min, m/z of 180), (1Z,5Z)-cyclododeca-1,5-diene (CDDE-diene) (5.93 min, m/z of 176), (Z)-cyclododecene (CDDE) (7.97 min, m/z of 178), 2-dodecene (6.61 min, m/z of 180), and formaldehyde (2.82 min, m/z of 31), which can be detected in the downstream products. Table S6 and Fig. S2 present the specific mass spectrometric information. Three intermediates (D-gluconate, 3-hydroxypropanoic, and formaldehyde) were proposed to enter the TCA cycle by forming acetyl-SCoA and succiny-CoA, because the functional enzymes of alcohol dehydrogenase (YiaY), salicylate hydroxylase (Slhe), and galactonate dehydratase (GanD) were detected during the degradation process [30-32]. Considering that 3-hydroxypropanoic and formaldehyde were identified, it could be deduced that they were converted to 2-oxoglutaratc and acetaldehyde when the reactions were catalyzed by Slhe and YiaY, respectively. Similar to other reports, 2-oxoglutaratc was converted by alpha-oxoglutarate dehydrogenase (SucA) to succinyl-SCoA, which is a precursor to TCA cycle, and then to CO_2 and H_2O [33].

The other pathway was the substitution of bromine atoms by hydroxylation of HBCD to form 9-boraneyl-2,5,6,10-tetrabromocyclododecan-1-ol (PBCD-ols) (5.18 min, m/z of 591), 6-boraneyl-5,9,10-tribromocyclododecane-1,2-diol (TetrBCD-diols) (6.67 min, m/z of 528), 2,6,10-tribromocyclododecane-1,5,9-triol (TriBCD-triols) (6.25 min, m/z of 465), and others. HBCD-degrading strains IP26 [11], HS9 [34], and GJY [9] have similar pathways. These strains' debromination capability on HBCD and some bromo products via hydroxyl substitution was due to the action of functional proteins, such as LinB [14], DhaA [24], GST [35], and CYP450 [27]. During the debromination pathway in this study, three enzymes (DhaA, LinB, and GST) were upregulated by 1.4-, 1.6-, and 2.0-fold, respectively. CYP450 was downregulated and may not be fully involved in the debromination of HBCD. This finding was partly different from the previous description of GST and CYP450, which reportedly participate in the debromination reaction during the degradation of HBCD [35].

The typical product of TriBCD-triols might undergo ring-cleavage to transform 4-bromobutan-1-ol (BMBTL) through oxygenases, such as quercetin 2,3-dioxygenase (QDGE) and monooxygenase (MOGE) [36, 37]. These oxygenases may be responsible for the conversion of TetrBCD-diols to 5-bromohexane-1,4-diol (BHEDL) [38, 39]. The key chemical reactions catalyzed by these oxidative enzymes with a broad range of substrates are hydroxylation and epoxidation [40]. 4-BBA and other intermediate products decomposed to form succinyl-SCoA and oxaloacetate into TCA cycle by alka monooxygenase alpha chain (LuxA), YiaY, and DhaG, which were upregulated by 3.2-, 1.2-, and 2.0-fold, respectively. The abundance of DhaG increased by more than 2-fold in the process of HBCD degradation. Surprisingly, the gene *dhaG* that encoded DhaG was not found in genome sequences, but DhaG was found in 11 upregulated proteins (Fig. 3d). A new gene encoding DhaG–hypothetical gene (*HBCD-hd-1*) may exist in strain Y3. Its function will be verified in a subsequent section.

Comparative genomic analysis and gene arrangement

By phylogenic analysis, strain Y3 was most closely related to *Acinetobacter venetianus* JKSF02 based on 16S rRNA genes (Fig. S3), whereas it was most closely related to *S. indicum* B90A with a similarity of 81.65% based on the whole genome, as previously reported for HBCD-degrading bacteria (Fig. 5a and Table S2). Comparative genomic mapping showed a complete synteny conservation between strains Y3 and B90A (Table S2 and Fig. 5b). However, the average amino acid identity (AAI) between the two strains was only 42.39% (Fig. S4). According to the species classification criteria of AAI (95%–96%) [41], strains F2 and IP 26 may be the same species, whereas strain Y3 was distantly related to other HBCD-degrading strains in the phylogenic analysis (Fig. S3).

The degrading enzymes were encoded by functional gene clusters, as shown in the Fig. 5c. Three key dehalogenation genes (*linA*, *linB*, and *dhaA*) [42-44] and other major potential biodegradation genes (*gst*, *cyp450, yiaY*, *frmA*, and *catB*) [26, 27, 31, 45, 46] were found in the gene cluster of strain *Citrobacter sp*. Y3. The expressions of all enzymes encoded by these genes were upregulated to different extents in HBCD-treatment groups. The other eight strains contained only some of the key dehalogenation genes. Strains HBCD-sjtu contained only *dhaG*. Strains F2 and *A. venetianus* JKSF02 contained only genes *dhaA*, *linA*, and *dhaG*. Notably, strain Y3 contained multiple dehalogenation genes, thereby indicating its more powerful potential for the efficient degradation of HBCD.

Most of the reported HBCD-degrading bacteria contained *linA*, whereas only strains Y3 and B90A harbored *linB.* A coordinated gene *linC* was found in the upstream of *linA* in four strains (B90A, P25, F2, and TKS). The *linC*, also named *P-450lin*, was a member of the *cyp450* gene family [47]. Enzyme LinC encoded by *linC* was responsible for electron transfer and substrate binding, and it cooperated with LinA to replace bromine with hydroxy [48]. However, the genes of strain Y3 coordinated with linA responsible for debromination was different with other strains. The upstream of *linA* was a single operon composed of *purH* and *purD* [49]. Based on the Paul W. Sternberg operon hypothesis, the demand for gene expression machines for gene expression can be minimized by operons [50]. It may contribute to a higher expression of LinA, because findings were consistent with the nearly 2-fold increase of LinA expression in

protein analysis. The same situation was found for the *catB*, *pcag*, and *frma* genes in strain Y3. Although *yiaY*, *pobA*, and *catB* were found in the downstream of the *gst* in four strain genomes (B90A, F2, and TKS), their gene sequences and arrangement were totally different. Genes *trspE* (coding transposase) and *resA* (coding resolvase), which were closely related to *dhaA*, were also found in four strains, namely, TKS, F2, IP26, and B90A. The genes were almost always adjacent to each other on the chromosome and formed defined secondary metabolite gene clusters [51]. However, *trspE* and *resA* were not found in the upstream and downstream of *dhaA* in strain Y3. Instead, *ygfk* and *ygfM* were found, and these encoded molybdate-containing enzymes and polypeptides carrying the FAD domain, respectively. They can mediate electron transfer in a wide variety of metabolic reactions, which may be more conducive to the participation of *dhaA* in the dehalogenation process in the degradation of HBCD [51]. By genomic annotation, the *dhaG* gene was not found in strain Y3, but enzyme DhaG was sharply upregulated after HBCD treatment. By genome mapping, DhaG corresponded to a hypothesis gene, which indicated that the gene (named *HBCD-hd-1*) might be a new gene encoding DhaG. To further explore the homology of *HBCD-hd-1* and *dhaG*, *dhaG* sequences from 44 bacteria were selected from NCBI and compared with the *HBCD-hd-1* using NJ phylogenetic tree analysis (Fig. S5). The *HBCD-hd-1* had low homology with the reported *dhaG* sequences, including those from B90A and P25. These results were consistent with the results of gene cluster analysis.

Verification of HBCD and its intermediate degradation by key enzyme encoded by *HBCD-hd-1*

The *HBCD-hd-1* gene with a size of 2550 bp was successfully cloned and heterologously expressed in *E. coli* (Fig. 6a). The results of first-generation sequencing of *E. coli* are presented in Table S7. The recombinant *E. coli* could sharply transform HBCD with 100% removal rate within 3 days of treatment (Figs. 6b and c). The removal efficiency by recombinant *E. coli* was much faster than that by strain Y3, indicating that a higher concentration of functional enzyme showed stronger degradation performance. Meanwhile, about 7.1 mg/L of bromine ion was generated, and the production reached a plateau after 3 days. Theoretically, six Br^- was produced when one HBCD was completely debrominated. The ratio of the detected Br^- concentration divided by the theoretically transformed Br^- concentration could serve as a marker of debromination. In the present study, about 98.61% HBCD were completely debrominated. Like other haloacid dehalogenases, the enzyme encoded by *HBCD-hd-1* gene could debrominated a typical mother compound of 4-BBA (Figs. 6e and f) with the peak appearing at a retention time of 3.1 mins with an iron at m/z 167 in ESI negative mode. After 4 d of treatment, the concentration of 4-BBA obviously decreased with the gradual increase in the concentration of 4-hydroxybutanoic acid (4-HDBA) (m/z of 104) (Figs. 6g and h). A similar functional description was presented previously [23, 52]. The results verified for the first time that haloacid dehalogenase encoded by a new functional gene *HBCD-hd-1* not only transforms 4-BBA to 4-HDBA but also efficiently degrades HBCD (including α-, β-, and γ-HBCD) in just 2 days. The performance was sharply faster than the performance obtained by using other strains.

Conclusions

Several isolates from the genus of *Citrobacter* have been reported to degrade environmental pollutants, such as 2,4,6-trinitrotoluene [53], polyethylene, plastic mixtures [54], textile dye [55], and radioactive pollutants [56]. They have the degradation potential to treat a wide range of environmental pollutants. They can reproduce and develop in a barren environment. They can efficiently degrade HBCD and use it as sole carbon source. Their use can eventually lead to the complete mineralization of HBCD without secondary contamination. They deserve more attention because of their good potential for use in treating HBCD and other compounds with similar structure in the natural environment, especially in low-nutrient soils and water. Six key genes and their corresponding encoded proteins that were responsible for dehalogenation were obviously upregulated. The strain Y3 contained more abundant and effective genes for debromination. Furthermore, a new functional gene *HBCD-hd-1* that encoded DhaG was verified to degrade HBCD (including α-, β-, and γ-HBCD) for the first time. Results confirmed that this was a new dehalogenation gene. The identification of this enzyme may provide new perspectives and ideas for researchers focusing on the removal of HBCD in the environment.

Methods

Chemicals, reagents, and bacterial strain. HBCD (99% in purity) and its three diastereomers with ^{13}C-HBCD (α-, β-, and γ-HBCD, 99% in purity) were used as target compounds and purchased from Sigma Chemical, Co. (St Louis, MO, USA). It was dissolved in acetone to yield a stock solution (1000 mg/L). After filtration via a 0.22 μm nylon membrane, the stock solution was added into the mineral media to obtain the desired concentrations. 4-BBA (98%) was obtained from Aladdin Biochemical Technology, Co. (Shanghai, China). All solvents and reagents used in this study were of HPLC grade and purchased from Merck Company (Darmstadt, Germany). *Citrobacter* sp. Y3 was previously isolated from activated sludge obtained from a wastewater treatment plant in an electronic industrial park [19]. DNA maker, clone vector pEASY-T1, vector pCold-, endonuclease NdeI and XbaI, Competent Cell DH5α, and *Escherichia coli* BL21 (DE3) were bought from Beijing TransGen Biotech, Co. (Beijing, China). PCR primers were obtained from Sangon Biotech, Co. (Shanghai, China).

Batch biodegradation experiments. Experiments for product analysis were conducted, in which three diastereomers of ^{13}C-HBCD served as the sole carbon sources (10 mg/L). The sample was collected at many different reactive times and then centrifuged at 7,000 rpm for 5 min to obtain the supernatant. To obtain better product analysis results, the sample was extracted and concentrated; the details of the specific method are presented in the Supporting Information [57]. To detect $^{13}CO_2$, the experimental conditions and settings used were completely consistent with the batch experiment, and the vacuum sampling bag was used to collect the gas (60 ml) produced by the reaction system daily from 1 d to 6 d. All experiments were performed in triplicate, and the average value with standard deviation (error bar) was obtained.

Chemical analytical. The HBCD concentration was analyzed by LC-MS/MS (Trip Quad 5500, SCIEX, Singapore). The gradient elution method was adopted, and the mobile phase consisted of water (10%) and acetonitrile (90%). The flow rate was 0.3 mL/min. The injection volume was 5 μL and the total elution

time was 6 min for each sample. The collected extract was injected into UPLC-Q-TOF-MS (Agilent 1290, Palo Alto, CA, United States; Bruker, Germany) using electrospray ionization (ESI) in both positive and negative modes to identify the major degradation products of HBCD and 4-BBA. The $^{13}CO_2$ produced by ^{13}C-HBCD (α-, β-, and γ- HBCD) mineralization was detected by high-precision laser isotope analyzer (Picarro L2130i, USA). The detection mode was set to $^{13}CO_2$, $^{12}CO_2$-dry, and H_2O. Before testing, the tested gas and N_2 were mixed at a ratio of 9:1 in the vacuum gas sampling bag. Bromide ions were detected by ion chromatography (Metrohm model 733, Herisau, Switzerland).

DNA and protein extraction. DNA was extracted by using a DNA extraction kit (TIANGEN, China), and the concentration and purity of DNA samples were detected by using a spectrophotometer (Thermo, Nanodropone, USA). The protein was extracted by centrifugation to collect bacteria and rinsed quickly with precooled PBS 2–3 times to avoid bacterial contamination. After each cleaning, the supernatant was completely discarded by 5000 g centrifugal 5 min at 4 ℃, and the bacteria were collected in 1.5 mL centrifuge tube (frozen tube). The volume of bacteria was recorded, and they were stored in refrigerator at -80 ℃ after quick freezing with liquid nitrogen.

Genome sequencing, assembly, and analysis. The whole genome sequence of strain *Citrobacter* sp. Y3 was prepared and completed. The library was sequenced using PacBio RS to obtain clean data and reads that can be used for analysis. These reads were assembled using SMTR portal (v2.0). Open reading frames (ORFs) were predicted using Prodigal (v2.60) [58]. The completeness and contamination were estimated by CheckM [59]. The whole genome of *Citrobacter* sp. Y3 was uploaded to GenBank with the accession number GCA011602505.1.

Proteomic analyses. The mass spectrometry analysis of label-free quantitative proteome was completed by Thermo fusion mass spectrometry. The raw data files were processed with MaxQuant v.1.6.1.0 to search the database and for quality control [60]. The positive and negative mixed library search strategy was adopted. The false positive rate of the peptide was estimated to be 0.01, and the protein was quantitatively analyzed by label-free quantitative analysis. Proteins were considered differentially expressed when they exhibited at least 1.5-fold change in abundance between treatment and reference proteomes. Proteins were mapped into metabolic pathways using Kyoto Encyclopedia of Genes and Genomes (KEGG) [61]. The mass spectrometry proteomics data have been deposited to the ProteomeXchange with the dataset identifiers (PXD033344).

Fuctional verification of gene HBCD-hd-1. The *HBCD-hd-1* gene was expressed and purified in *E. coli*, and the degradation of 4-BBA was carried out. After enrichment and culture of strain Y3, the DNA was extracted by DNA extraction kit, and the DNA fragment of *HBCD-hd-1* was amplified with primers 2448-F and 2448-R (Table S1). Then, the *HBCD-hd-1* gene was cloned and ligated into the cloning vector pEASY-Simple. The plasmid was transformed and expressed in DH5α competent cells and extracted by plasmid extraction kit. The plasmids and pCold-□ vectors were digested with NdeI and XbaI for 1 h at 37 ℃, respectively. After recovery and purification, the target gene *HBCD-hd-1* was ligated with an empty vector with the T4 ligase (16 ℃, 12 h). *E. coli* harboring *HBCD-hd-1* was grown in LB culture at 37°C to an OD_{600}

of 0.6–0.8 and subsequently induced for 12 h by adding 0.1 mM isopropyl-beta-D-thiogalactopyranoside at 16°C. Electrophoresis and sequencing were performed to detect the gene sequence of *HBCD-hd-1* and to ensure that no mutation occurred. After expanded culture, batch experiments were carried out with 4-BBA to verify the debromination function of *HBCD-hd-1*. Functional genes *HBCD-hd-1* was uploaded to NCBI with the accession number ON155918.

Analytical methods. On the basis of genomic and proteomic analysis, the expressions of genes involved in the degradation process were detected and screened out as differentially expressed genes (DEGs). Enrichment analysis of DEGs from the three groups was performed to illustrate their distribution on the KEGG pathways. This helped elucidate their possible functions in the biological process and pathway. The phylogenetic tree of the whole genome was drawn by GTDB-Tk [62]. The data of average amino acid identity (AAI) and 16S rRNA gene identity were analyzed by CompareM [63]. The gene cluster arrangements were based on the length of functional genes. The phylogenetic tree of functional genes was generated by Neighbor Joining method [64]. Evolutionary distance bootstrap values were determined using the bootstrap method on MEGA-X [65]. To analyze the specific differences among several kinds of strain, genetic sequence alignment was made by using the sequence comparison tool, DNAMAN, and visualized through Circos [66].

Declarations

Author contributions

Xingxing Peng: Original draft writing, Experiment conducting, Data analysis, Software, Visualization, Research design, Supervision. Tianyu Li: Experiment conducting, Data analysis, Visualization, Revision. Qihang Zheng: Original draft writing, Experiment conducting, Data analysis, Software, Visualization. Yingyuan Lu: Experiment conducting, Data analysis. Yuzhe He: Experiment conducting, Data analysis. Yetao Tang: Research design, Supervision. Rongliang Qiu: Review & editing.

Funding

This work was financially supported by the National Natural Science Foundation of China (no. 42077128), the Pearl River Nova Program of Guangzhou (no. 201806010100).

Availability of data materials

The whole genome of Citrobacter sp. Y3 was uploaded to GenBank with the accession number GCA011602505.1. The mass spectrometry proteomics data have been deposited to the ProteomeXchange with the dataset identifiers (PXD033344). Functional genes HBCD-hd-1 was uploaded to NCBI with the accession number ON155918.

Ethics approval and consent to participate

Not applicable

Consent for publication

Not applicable

Competing interests

The authors declare that they have no known competing financial interests or personal relationships that could have appeared to influence the work reported in this paper.

Author details

[1] School of Environmental Science and Engineering, Sun Yat-sen University, Guangzhou 510006, Guangdong, China.[2] Guangdong Provincial Key Laboratory of Environmental Pollution Control and Remediation Technology, Sun Yat-sen University, Guangzhou 510275, China.[3] Guangdong Provincial Key Laboratory of Agricultural & Rural Pollution Abatement and Environmental Safety, College of Natural Resources and Environment, South China Agricultural University, Guangzhou 510642, China.[4] Guangdong Laboratory for Lingnan Modern Agriculture, South China Agricultural University, Guangzhou 510642, China

References

1. Zhang, Y. et al. Transport of hexabromocyclododecane (HBCD) into the soil, water and sediment from a large producer in China. *Sci. Total Environ*. 2017; 610: 94-100.
2. Cheng, H., Luo, H., Hu, Y. & Tao, S. Release kinetics as a key linkage between the occurrence of flame retardants in microplastics and their risk to the environment and ecosystem: A critical review. *Water Res.* 2020; 185.
3. Greaves, A. K. & Letcher, R. J. Comparative body compartment composition and in ovo transfer of organophosphate flame retardants in north american great lakes herring gulls. *Environ. Sci. Technol.* 2014; 48, (14): 7942-7950.
4. Li, D., Zhu, X., Zhong, Y., Huang, W., & Peng, P. Abiotic transformation of hexabromocyclododecane by sulfidated nanoscale zerovalent iron: Kinetics, mechanism and influencing factors. *Water Res.* 2017; 121: 140-149.
5. Beach, M. W. et al. Stability assessment of a polymeric brominated flame retardant in polystyrene foams under application-relevant conditions. *Environ. Sci. Technol.* 2021; 55, (5): 3050-3058.
6. Yu, F. et al. Microbial debromination of hexabromocyclododecanes. *Appl. Microbiol. Biotechnol.* 2021; 105, (11): 4535-4550.
7. Davis, J. W., Gonsior, S., Marty, G. & Ariano, J. The transformation of hexabromocyclododecane in aerobic and anaerobic soils and aquatic sediments. *Water Res.* 2005; 39, (6); 1075-1084.
8. Shah, S. et al. Complete genome sequence of *Bacillus* sp. HBCD-sjtu, an efficient HBCD-degrading bacterium. *3 Biotech*, 2018; 8, 291.

9. Geng, J., Han, M., Yang, X. & Li, Y. Bartlam, M.; Wang, Y., Different biotransformation of three hexabromocyclododecane diastereoisomers by *Pseudomonas* sp. under aerobic conditions. *Chem. Eng. J.* 2019; 374: 870-879.
10. Huang, L. et al. The HBCDs biodegradation using a *Pseudomonas* strain and its application in soil phytoremediation. *J. Hazard. Mater.* 2019; 380.
11. Heeb, N. V., Grubelnik, A., Geueke, B., Kohler, H. P. E. & Lienemann, P., Biotransformation of hexabromocyclododecanes with hexachlorocyclohexane-transforming *Sphingobium chinhatense* strain IP26. *Chemosphere.* 2017; 182: 491-500.
12. Peng, X. et al. Study of novel pure culture HBCD-1, effectively degrading Hexabromocyclododecane, isolated from an anaerobic reactor. *Bioresour. Technol.* 2015; 185: 218-224.
13. Heeb, N. V. et al. Stereochemistry of enzymatic transformations of (+)β- and (-)β-HBCD with LinA2-A HCH-degrading bacterial enzyme of *Sphingobium indicum* B90A. *Chemosphere.* 2015; 122: 70-78.
14. Heeb, N. V. et al. Kinetics and stereochemistry of LinB-catalyzed delta-HBCD transformation: Comparison of in vitro and in silico results. *Chemosphere.* 2018; 207: 118-129.
15. Shah, S. et al. Computational and in vitro analysis of an HBCD degrading gene DehHZ1 from strain HBCD-sjtu. *J. Biol. Reg. Homeos. Ag.* 2019; 33, (1): 157-162.
16. Heeb, N. V. et al. LinA2, a HCH-converting bacterial enzyme that dehydrohalogenates HBCDs. *Chemosphere.* 2014; 107: 194-202.
17. Schilling, I. E. et al. Kinetic isotope effects of the enzymatic transformation of gamma-hexachlorocyclohexane by the lindane dehydrochlorinase variants LinA1 and LinA2. *Environ. Sci. Technol.* 2019; 53, (5): 2353-2363.
18. Heeb, N. V., Zindel, D., Geueke, B., Kohler, H. E. & Lienemann, P. Biotransformation of hexabromocyclododecanes (HBCDs) with LinB-An HCH-converting bacterial enzyme. *Environ. Sci. Technol.* 2012; 46, (12): 6566-6574.
19. Peng, X. et al. Kinetics, pathways and toxicity of hexabromocyclododecane biodegradation: Isolation of the novel bacterium *Citrobacter* sp. Y3. *Chemosphere.* 2021; 274.
20. Peck, A. M. et al. Hexabromocyclododecane in white-sided dolphins: Temporal trend and stereoisomer distribution in tissues. *Environ. Sci. Technol.* 2008; 42, (7): 2650-2655.
21. Heeb, N. V. et al. Regio- and stereoselective isomerization of hexabromocyclododecanes (HBCDs): Kinetics and mechanism of β-HBCD racemization. *Chemosphere***,** 2008; 73: 1201-1210.
22. Koppen, R., Becker, R., Jung, C. & Nehls, I. On the thermally induced isomerisation of hexabromocyclododecane stereoisomers. *Chemosphere.* 2008; 71, (4): 656-662.
23. Wang, Y. Y., Feng, Y. B., Cao, X. P., Liu, Y. H. & Xue, S. Insights into the molecular mechanism of dehalogenation catalyzed by D-2-haloacid dehalogenase from crystal structures. *Scientific Reports.* 2018; 8.
24. Verschueren, K.; Seljée, F.; Rozeboom, H. J.; Kalk, K. H. & Dijkstra, B. W. Crystallographic analysis of the catalytic mechanism of haloalkane dehalogenase. *Nature.* 2018; 363, (6431): 693-698.

25. Dogra, C. et al. Organization of *lin* genes and IS6100 among different strains of hexachlorocyclohexane-degrading *Sphingomonas paucimobilis*: Evidence for horizontal gene transfer. *J. Bacteriol.* 2004; 186, (8): 2225-2235.
26. Ronen, Z. & Abeliovich, A. Anaerobic-aerobic process for microbial degradation of tetrabromobisphenol A. *Appl. Environ. Microb.* 2000; 66, (6): 2372-2377.
27. Rittle, J. & Green, M. T. Cytochrome P450 compound I: capture, characterization, and C-H bond activation kinetics. *Science.* 2010; 330, (6006): 933-937..
28. Zhong, Y. et al. Diastereoisomer-Specific biotransformation of Hexabromocyclododecanes by a mixed culture containing *Dehalococcoides mccartyi* Strain 195. *Front. Microbiol.* 2018; 9: 1713.
29. Heeb, N. V. et al. Lienemann, P., Stereochemistry of LinB-catalyzed biotransformation of delta-HBCD to 1R,2R,5S,6R,9R,10S-pentabromocyclododecanol. *Chemosphere.* 2013; 90, (6): 1911-1919..
30. Costa, D. M. A. et al. Brandao, T. A. S., Catalytic mechanism for the conversion of salicylate into catechol by the flavin-dependent monooxygenase salicylate hydroxylase. *Int. J. Biol. Macromol.* 2019; 129: 588-600.
31. Pony, P., Rapisarda, C., Terradot, L., Marza, E. & Fronzes, R. Filamentation of the bacterial bi-functional alcohol/aldehyde dehydrogenase AdhE is essential for substrate channeling and enzymatic regulation. *Nat. Commun.* 2020; 11, (1)
32. Babbitt, P. C. et al. A functionally diverse enzyme superfamily that abstracts the alpha protons of carboxylic acids. *Science.* 1995; 267, (5201): 1159-1161.
33. Yu, K. et al. An integrated meta-omics approach reveals substrates involved in synergistic interactions in a bisphenol A (BPA)-degrading microbial community. *Microbiome.* 2019; 7.
34. Huang, L. et al. The HBCDs biodegradation using a *Pseudomonas* strain and its application in soil phytoremediation. *J. Hazard. Mater.* 2019; 380.
35. Li, Y., Wang, R., Lin, C., Chen, S. & Shih, Y. The degradation mechanisms of Rhodopseudomonas palustris toward hexabromocyclododecane by time-course transcriptome analysis. *Chem. Eng. J.* 2021; 425, (9): 130489.
36. Pazmino, D. E. T., Winkler, M., Glieder, A. & Fraaije, M. W. Monooxygenases as biocatalysts: Classification, mechanistic aspects and biotechnological applications. *J. Biotechnol.* 2010; 146, (1-2): 9-24.
37. Fusetti, F. et al. Crystal structure of the copper-containing quercetin 2,3-dioxygenase from *Aspergillus japonicus*. *Structure.* 2002; 10, (2): 259-268.
38. Hutchinson, J. P. et al. Structural and mechanistic basis of differentiated inhibitors of the acute pancreatitis target kynurenine-3-monooxygenase. *Nat. Commun.* 2017; 8: 15827.
39. Fuchs, G., Boll, M. & Heider, J. Microbial degradation of aromatic compounds - from one strategy to four. *Nature Reviews Microbiology.* 2011; 9, (11): 803-816.
40. Dubey, K. K., PunitKumar & KumarSingh, P. PratyooshShuklab, *Microbial Biodegradation and Bioremediation* 2014.

41. Konstantinidis, K. T. & Tiedje, J. M. Towards a genome-based taxonomy for prokaryotes. *J. Bacteriol.* 2005; 187, (18): 6258-6264.
42. Liu, Y. et al. Enantiomer and carbon isotope fractionation of alpha-hexachlorocyclohexane by *sphingobium indicum* strain B90A and the corresponding enzymes. *Environ. Sci. Technol.* 2019; 53, (15): 8715-8724.
43. Schilling, I. E., Bopp, C. E., Lal, R., Kohler, H. P. E. & Hofstetter, T. B. Assessing aerobic biotransformation of hexachlorocyclohexane isomers by compound-specific isotope analysis. *Environ. Sci. Technol.* 2019; 53, (13): 7419-7431.
44. Kumari, R. et al. Cloning and characterization of lin genes responsible for the degradation of hexachlorocyclohexane isomers by *Sphingomonas paucimobilis* strain B90. *Appl. Environ. Microb.* 2002; 68, (12): 6021-6028.
45. Barber, R. D., Rott, M. A. & Donohue, T. J. Characterization of a glutathione-dependent formaldehyde dehydrogenase from Rhodobacter sphaeroides. *J. Bacteriol.* 1996; 178, (5): 1386-1393.
46. Cosper, N. J., Collier, L. S., Clark, T. J., Scott, R. A. & Neidle, E. L. Mutations in catB, the gene encoding muconate cycloisomerase, activate transcription of the distal ben genes and contribute to a complex regulatory circuit in *Acinetobacter* sp strain ADP1. *J. Bacteriol.* 2000; 182, (24): 7044-7052.
47. Ropp, J. D.; Gunsalus, I. C. & Sligar, S. G. Cloning and expression of a member of a new cytochrome P-450 family: cytochrome P-450lin (CYP111) from Pseudomonas incognita. *J. Bacteriol*. 1993; 175, (18): 6028-6037.
48. Manickam, N., Mau, M. & Schlomann, M. Characterization of the novel HCH-degrading strain, Microbacterium sp ITRC1. *Appl. Microbiol. Biotechnol.* 2006; **69**, (5): 580-588
49. Aiba, A. & Mizobuchi, K. Nucleotide sequence analysis of genes *purH* and *purD* involved in the de novo purine nucleotide biosynthesis of *Escherichia coli*. J. Biol. Chem. 1989; 264.
50. Zaslaver, A., Baugh, L. R. & Sternberg, P. W. Metazoan operons accelerate recovery from growth-arrested states. *Cell.* 2011; 145, (6): 981-992.
51. Bebien, M., Kirsch, J., Mejean, V. & Vermeglio, A. Involvement of a putative molybdenum enzyme in the reduction of selenate by *Escherichia coli*. *Microbiol-Sgm.* 2002; 148: 3865-3872.
52. Kurihara, T., Esaki, N. & Soda, K. Bacterial 2-haloacid dehalogenases: structures and reaction mechanisms. *J. Mol. Catal. B-Enzym.* 2000; 10, (1-3): 57-65.
53. Liao, H.et al. The integrated analysis of transcriptome and proteome for exploring the biodegradation mechanism of 2, 4, 6-trinitrotoluene by *Citrobacter* sp. *J. Hazard. Mater.* 2018; 349: 79-90.
54. Brandon, A. M. et al. Biodegradation of polyethylene and plastic mixtures in mealworms (larvae of tenebrio molitor) and effects on the gut microbiome. *Environ. Sci. Technol.* 2018; 52, (11): 6526-6533.
55. Sunkar, S., Nachiyar, V. C. & Renugadevi, K. Citrobacter freundii mediated degradation of textile dye Mordant Black 17. *J. Water Process Eng.* 2015; 8: 28-34.

56. Lloyd, J. R. & Yong, P. Macaskie, L. E., Biological reduction and removal of Np(V) by two microorganisms. *Environ. Sci. Technol.* 2000; 34, (7): 1297-1301.
57. Huang, Z. et al. One-pot synthesis of diiron phosphide/nitrogen-doped graphene nanocomposite for effective hydrogen generation. *Nano Energy*. 2015; 12: 666-674.
58. Hyatt, D.et al. Prodigal: prokaryotic gene recognition and translation initiation site identification. *Bmc Bioinformatics.* 2010; 11.
59. Parks, D. H., Imelfort, M., Skennerton, C. T., Hugenholtz, P. & Tyson, G. W. CheckM: assessing the quality of microbial genomes recovered from isolates, single cells, and metagenomes. *Genome Res.* 2015; 25, (7): 1043-1055.
60. Cox, J. & Mann, M., MaxQuant enables high peptide identification rates, individualized p.p.b.-range mass accuracies and proteome-wide protein quantification. *Nat. Biotechnol.* 2008; 26, (12): 1367-1372.
61. Jones, P. et al. InterProScan 5: genome-scale protein function classification. *Bioinformatics.* 2014; 30, (9): 1236-1240.
62. Chaumeil, P. A., Mussig, A. J., Hugenholtz, P. & Parks, D. H. GTDB-Tk: a toolkit to classify genomes with the Genome Taxonomy Database. *Bioinformatics.* 2020; 36, (6): 1925-1927.
63. Kim, D., Park, S. & Chun, J. Introducing EzAAI: a pipeline for high throughput calculations of prokaryotic average amino acid identity. *J. Microbiol.* 2021; 59, (5): 476-480.
64. Lefort, V., Desper, R. & Gascuel, O. FastME 2.0: A comprehensive, accurate, and fast distance-based phylogeny inference program. *Mol. Biol. Evol.* 2015; *32*, (10): 2798-2800.
65. Kumar, S., Stecher, G., Li, M., Knyaz, C. & Tamura, K. MEGA X: molecular evolutionary genetics analysis across computing platforms. *Mol. Biol. Evol.* 2018; **35**, (6): 1547-1549.
66. Krzywinski, M. et al. Circos: An information aesthetic for comparative genomics. *Genome Res.* 2009; 19, (9): 1639-1645.

Figures

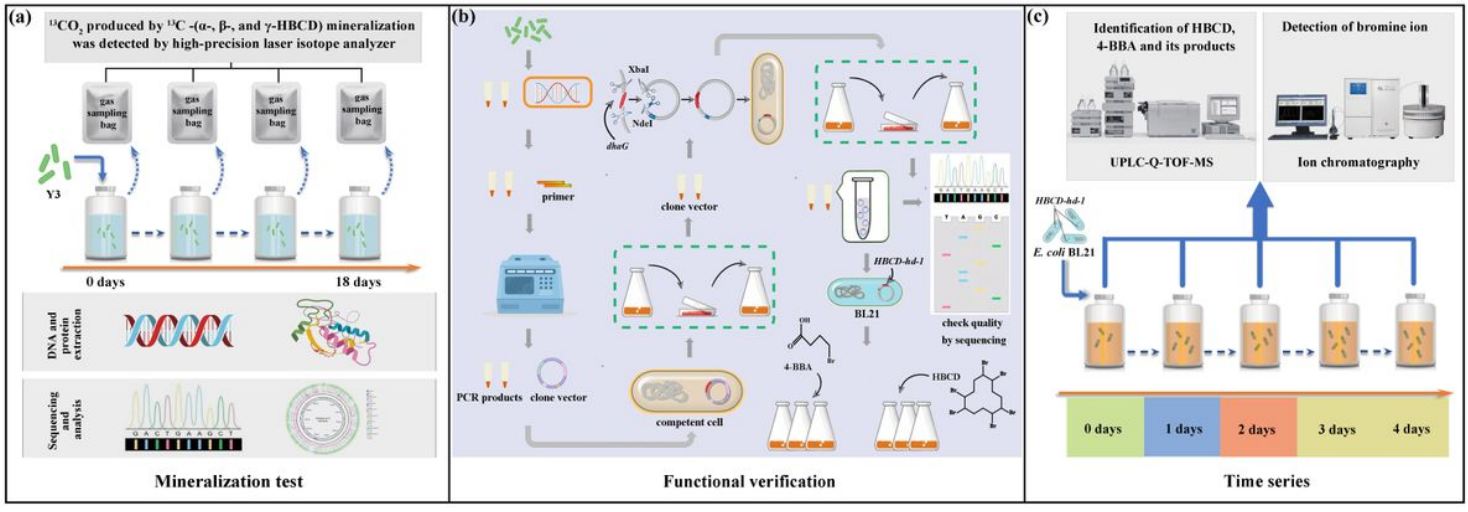

Figure 1

Experimental setup. (a) Determination of ^{13}C-HBCD usage by measuring $^{13}CO_2$ production in the presence of strain Y3; (b) Functional verification of key gene, including *HBCD-hd-1* gene clone and expression; (c) Degradation HBCD and its intermediates of 4-BBA by expressed proteins by recombinant *E. coli* BL21 containing *HBCD-hd-1* at different time points (0, 1, 2, 3, 4 days). Each experiment was conducted three replicates.

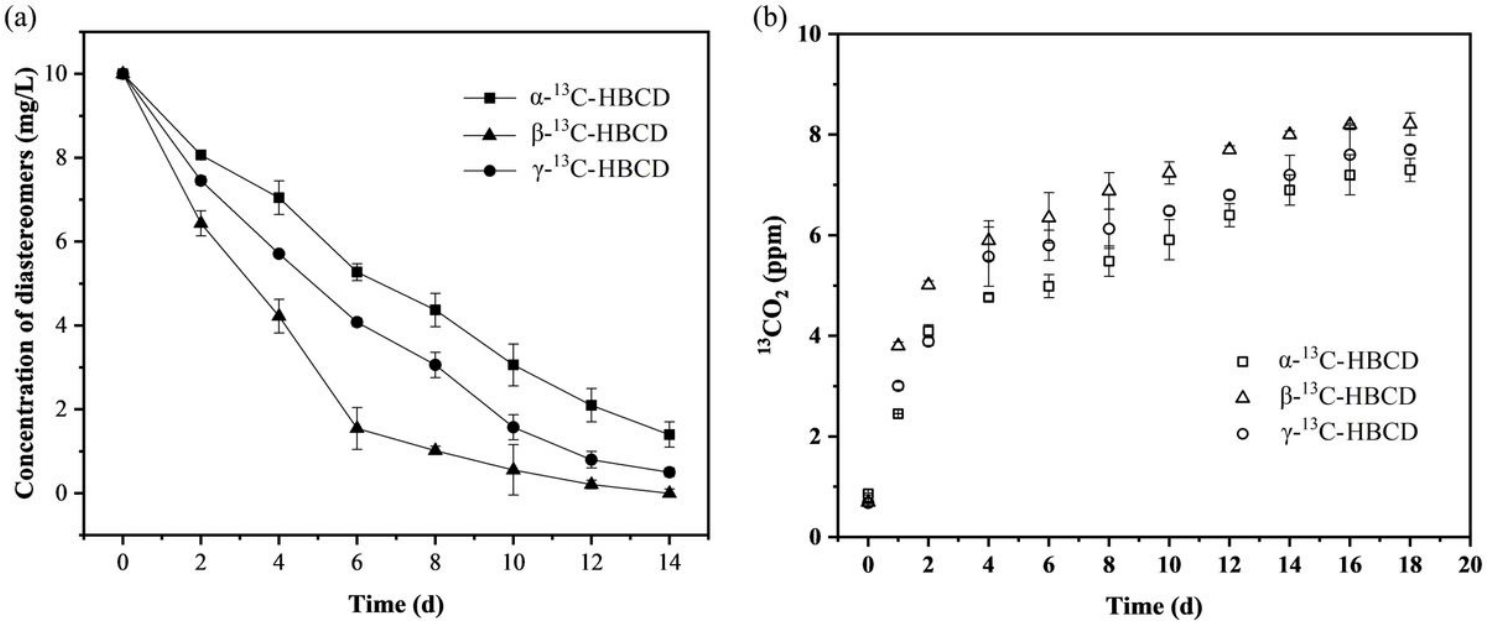

Figure 2

Mineralization of HBCD. (a) Concentration of the individual HBCD diastereomers (α-^{13}C-, β-^{13}C- and γ-^{13}C-HBCD) transformed by strain Y3; (b) Concentration of $^{13}CO_2$ produced by mineralization of three diastereomers (α-^{13}C-, β-^{13}C- and γ-^{13}C-HBCD).

(a)

Before/after reaction	Protein number	Remarks
Up regulated	492	Ratio>2,p-value<0.05
Down regulated	670	Ratio<0.5,p-value<0.05

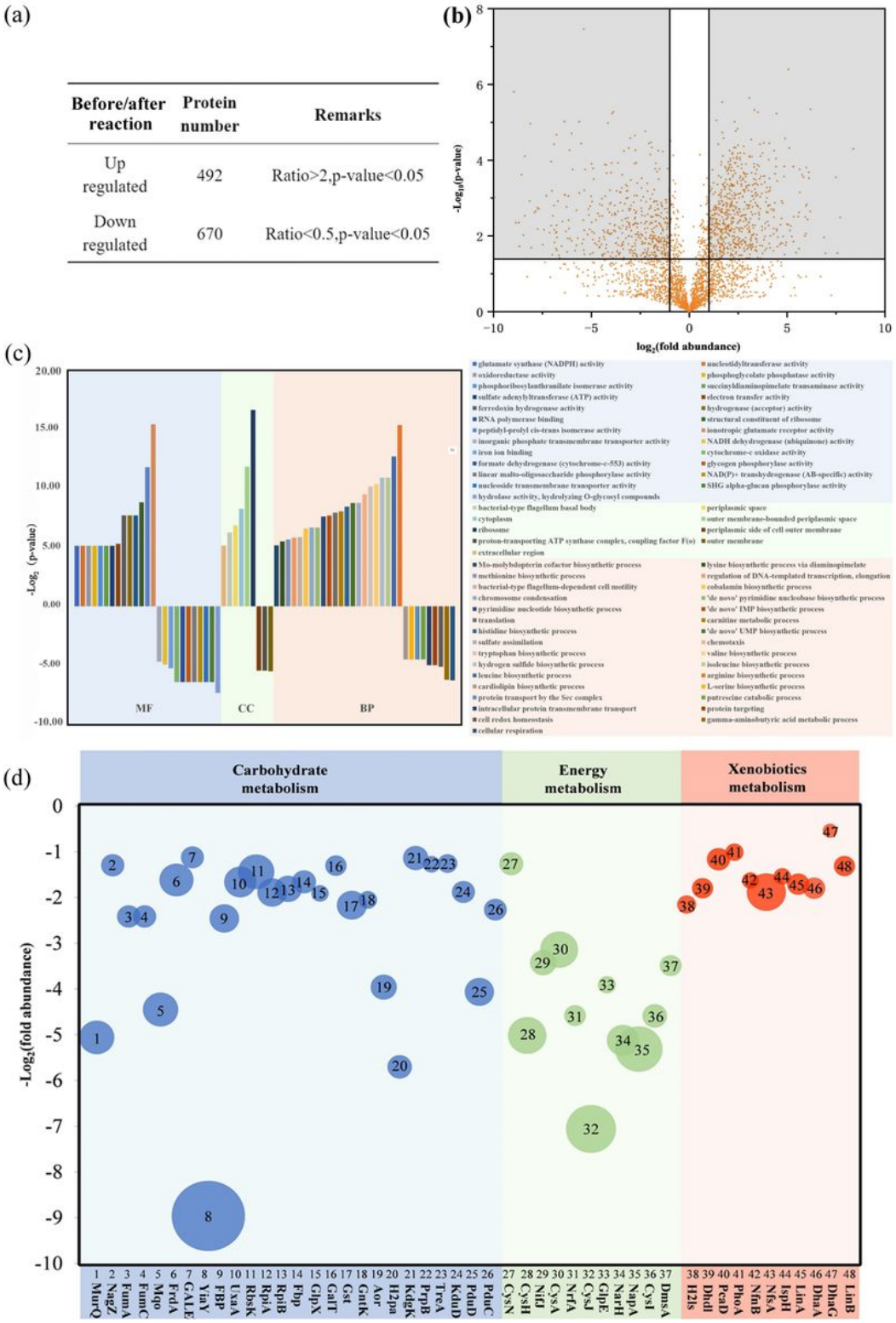

Figure 3

Proteomic analysis. (a) Protein statistics before and after reaction; (b) Volcano plot of quantified proteins of strain Y3, statistically significant ($p \leq 0.05$) differentially abundant proteins ($-1 \leq \log2$ (fold abundance) ≥ 1) are shaded gray; (c) All the identified protein classification diagram based on biological processes, cellular components and metabolic functions; (d) All the up-regulated protein classification bubble maps screened according to carbon metabolism, energy metabolism and xenobiotics metabolism.

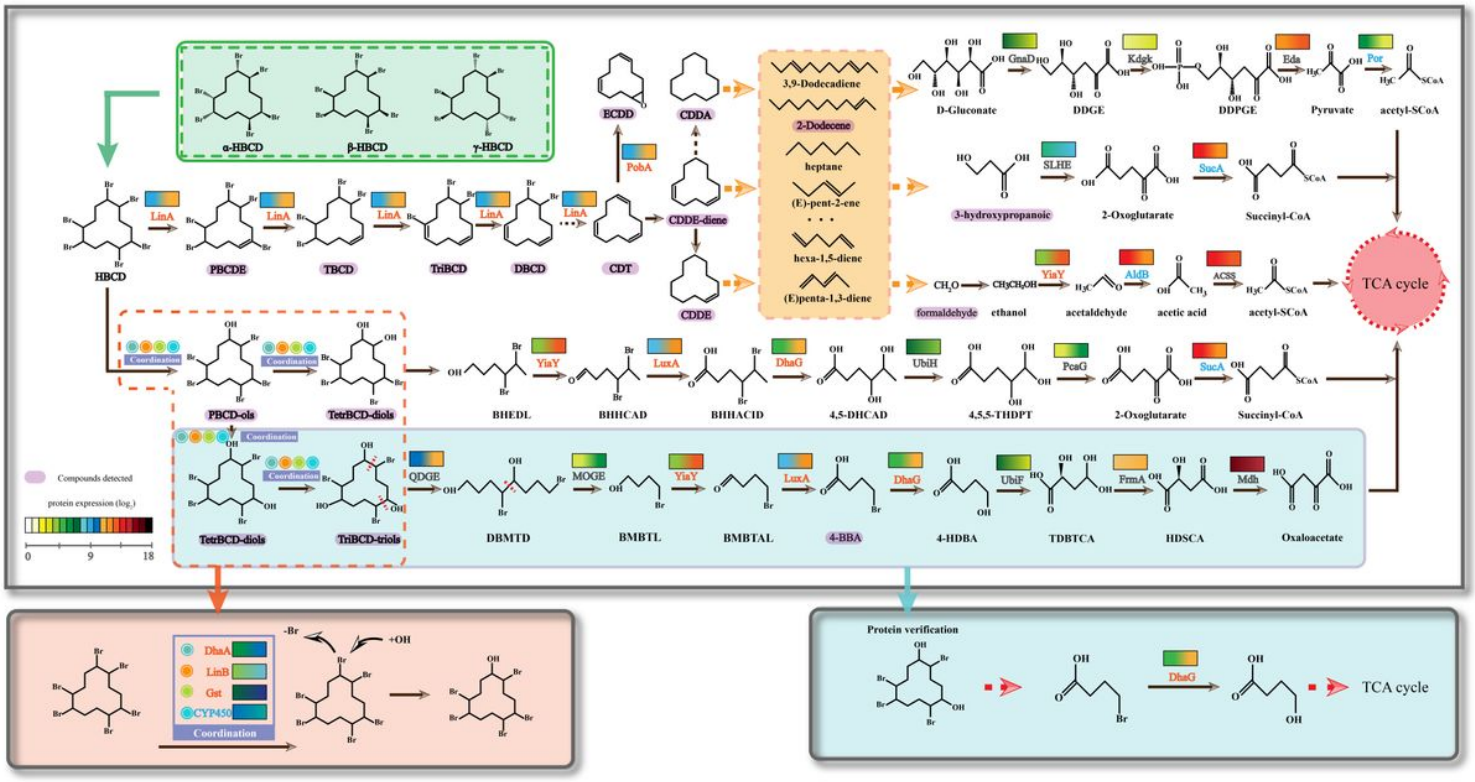

Figure 4

Reconstruction of HBCD-degrading pathway using metabolite analysis, functional annotation of genome, and proteomic analysis. The orange name indicated the up-regulated protein, the blue name indicated the down-regulated protein, and the black name means that the protein was neither up-regulated nor down-regulated. The intermediates marked in purple represent those that had been reported by previous references. The yellow dotted frame indicates the intermediates that possibly generated. Abbreviations, PBCDE, pentabromocyclododecane; TBCD, Tetrabromocyclododecane; TriBCD, tribromocyclododecane; DBCD, dibromocyclododecane; CDT, cyclododecatriene; ECDD, (4Z,8Z)-13-oxabicyclo [10.1.0] trideca-4,8-diene; CDDA, cyclododecane; CDDE-diene, (1Z,5Z)-cyclododeca-1,5-diene; CDDE, (Z)-cyclododecene; DDGE, ; DDPGE, ; PBCD-ols, 9-boraneyl-2,5,6,10-tetrabromocyclododecan-1-ol; TetrBCD-diols, 6-boraneyl-5,9,10-tribromocyclododecane-1,2-diol; TriBCD-triols, 2,6,10-tribromocyclododecane-1,5,9-triol; DBMTD, 4,8-dibromooctane-1,5-diol; BMBTL, 4-bromobutan-1-ol; 4-BBA, 4-bromobutyric acid; 4-HDBA, 4-hydroxybutanoic acid; TDBTCA, 2,4,4-trihydroxybutanoic acid; HDSCA, (S)-2-hydroxysuccinic acid; BHEDL, 5-bromohexane-1,4-diol; BHHCAD, 5-bromo-4-hydroxyhexanal; BHHACHD, 5-bromo-4-hydroxyhexanoic acid; 4,5-DHCAD, 4,5-dihydroxyhexanoic acid; 4,5,5-THDPT, 4,5,5-trihydroxypentanoic acid; The abbreviation of genes, LinA, gamma-hexachlorocyclohexane dehydrochlorinase; LinB, haloalkane dehalogenase LinB; DhaA, haloalkane dehalogenase; Gst, glutathione S-transferase; CYP450, cytochrome P450; PobA, p-hydroxybenzoate 3-monooxygenase; YiaY, alcohol dehydrogenase; QDGE, Quercetin 2,3-dioxygenase; MOGE, Monooxygenase; LuxA, alkanal monooxygenase alpha chain; DhaG, haloacid dehalogenase; UbiH, 2-octaprenyl-6-methoxyphenol hydroxylase; UbiF, 3-demethoxyubiquinol 3-hydroxylase; PcaG, protocatechuate 3,4-dioxygenase; FrmA, S-(hydroxymethyl)glutathione dehydrogenase; SucA, 2-oxoglutarate dehydrogenase E1 component; Mdh, malate dehydrogenase; AldB,

aldehyde dehydrogenase; ACSS, acetyl-CoA synthetase; Slhe, Salicylate hydroxylase; GanD, galactonate dehydratase; Kdgk, 2-dehydro-3-deoxygluconokinase; Eda, 2-dehydro-3-deoxyphosphogluconate aldolase; Por, pyruvate-ferredoxin/flavodoxin oxidoreductase.

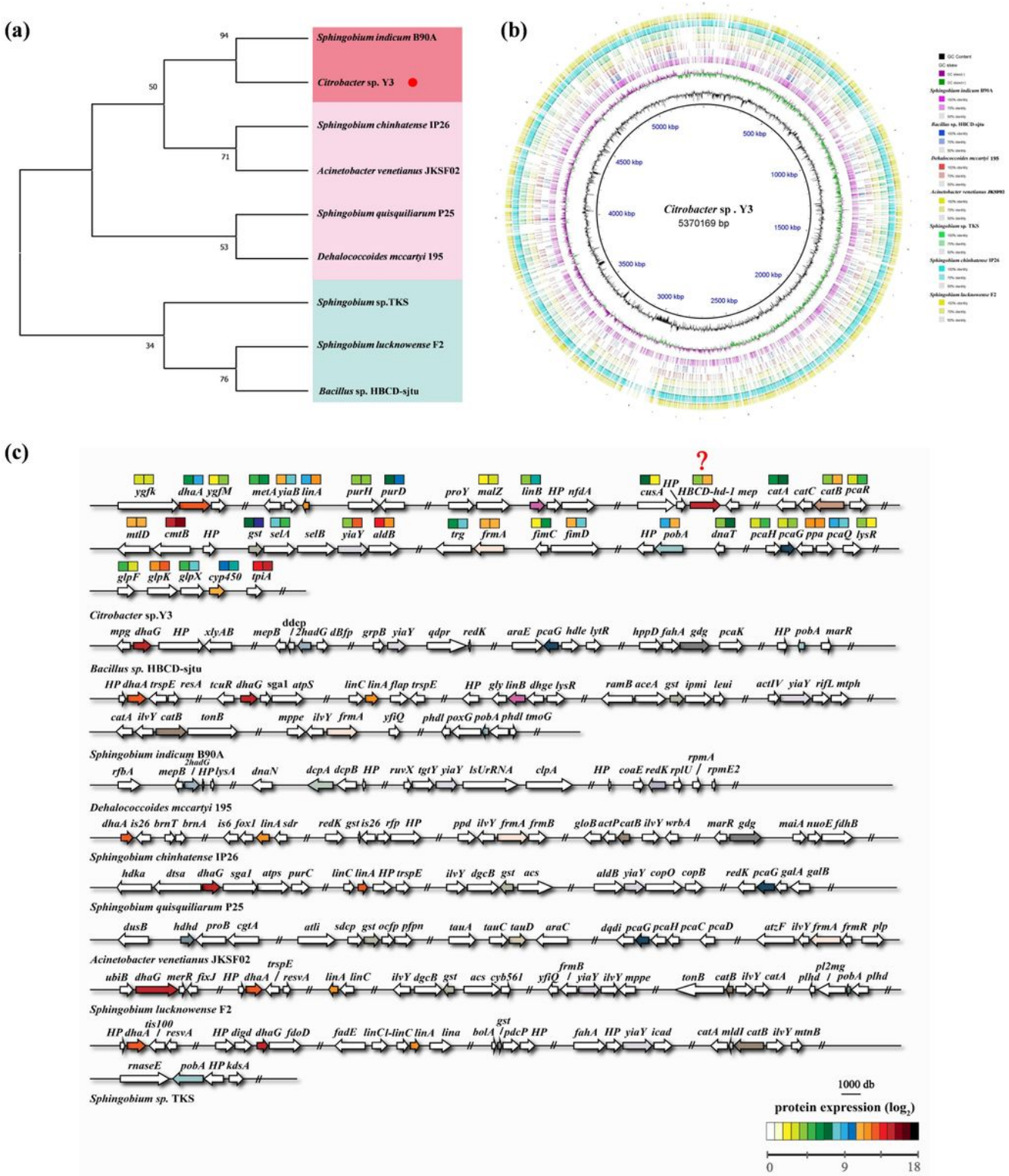

Figure 5

Genomic analysis of strain Y3. (a) Phylogenetic tree constructed from the whole genome of 9 HBCD-degrading strains, and the red dot marks the *Citrobacter* sp. Y3 in this experiment; (b) Comparative genomic characterization of Y3. Rings from inside to outside: track1, contig boundaries and plasmid (black) of Y3; track 2, GC content; track 3, GC skew; tracks 4–10, nucleotide alignment to Y3 with seven finished genomes of selected HBCD-degrading strains; (c) Gene arrangement of HBCD degradation genes. Genes with the same function are marked with the same color. Annotations are shown for *gst* (glutathione S-transferase), *yiaY* (alcohol dehydrogenase), *bdhAB* (butanol dehydrogenase), *tauD* (taurine dioxygenase), *catB* (muconate cycloisomerase), *pcaG* (Protocatechuate 3,4-dioxygenase), *frmA* (S-(hydroxymethyl) glutathione dehydrogenase), *adhE* (acetaldehyde dehydrogenase), *dhaG* (haloacid dehalogenase), *ALR2* (aldehyde reductase), *gdg* (Gentisate 1,2-dioxygenase), *dhaA* (haloalkane dehalogenase), *pobA* (Monooxygenase), *adh* (alcohol dehydrogenase), *HDHD* (haloacid dehalogenase-like hydrolase). A detailed information of genes is shown in Table S8.

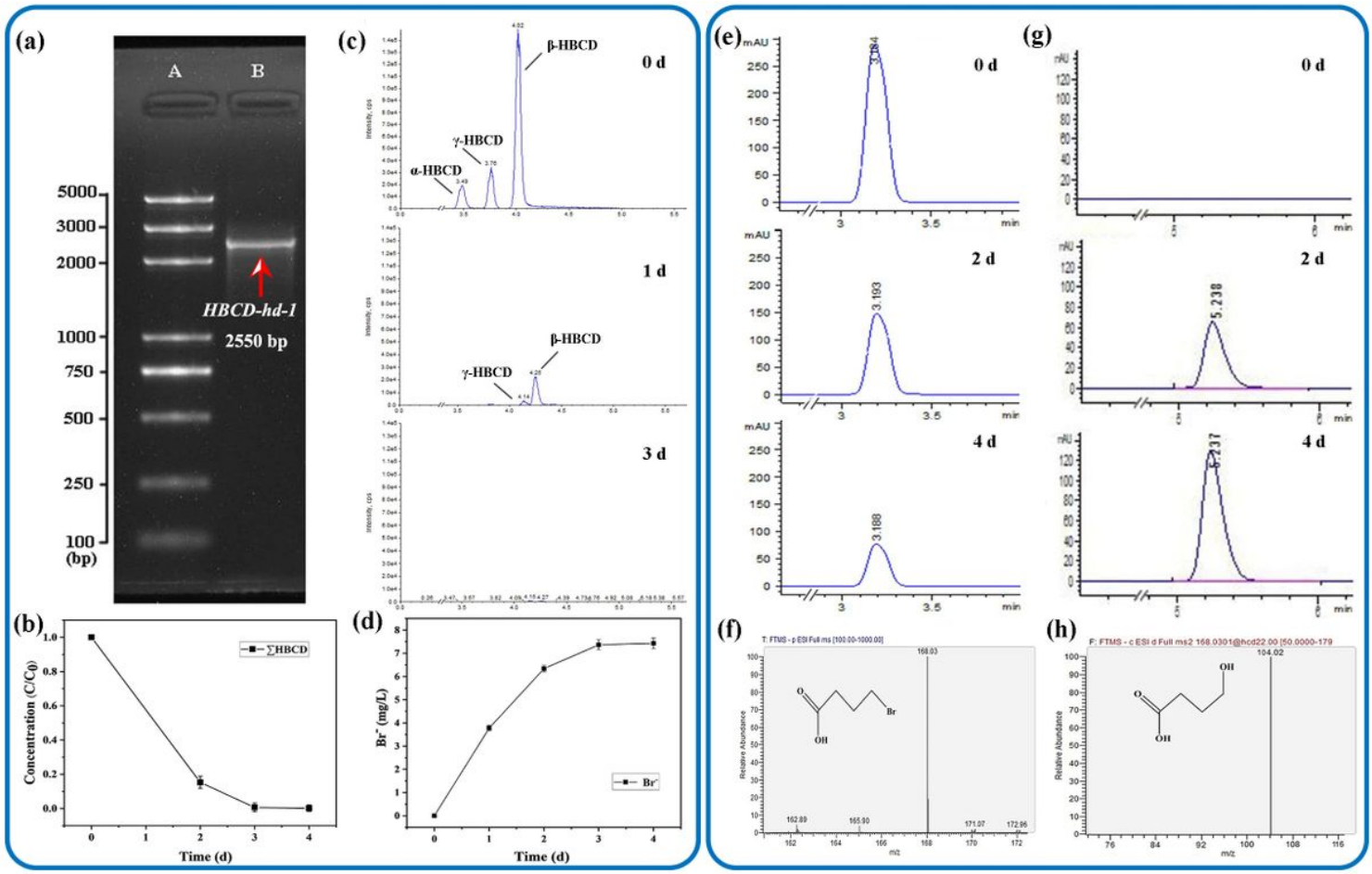

Figure 6

Functional verification of *HBCD-hd-1*. (a) Amplified DNA fragments after colony PCR analysis of *Citrobacter* Y3 *HBCD-hd-1*; (b) Degradation of ΣHBCD by recombinant *E. Coli* containing *HBCD-hd-1*; (c) Chromatograms of HBCD (including α-, β-, γ-HBCD) degraded by recombinant *E. Coli* during different times (0, 1, and 3 days); (d) Generation of bromine ion; (e) Chromatograms of 4-BBA degraded by recombinant *E. Coli* during different times (0, 1, and 3 days); (f) Mass spectrum of 4-BBA; (g)

Chromatograms of 4-HDBA generation during different degradation times (0, 1, and 3 days); (h) Mass spectrum of 4-HDBA.

Supplementary Files

This is a list of supplementary files associated with this preprint. Click to download.

- supportingiformation.docx